

Table I Accomplishment contents of each module

Module	Accomplishment Contents
Control Station Module	<ul style="list-style-type: none"> ▪Remotely speed and the direction command transmission ▪ Steering controller signal monitoring ▪Wheel/rail contact image acquisition using wireless camera systems
Steering Controller Module	<ul style="list-style-type: none"> ▪Generation of steering command to actuator based on the control algorithm ▪A/D and D/A input/output terminals ▪MATLAB/SIMULINK and dSPACE as a rapid control prototyper
Actuator Module	<ul style="list-style-type: none"> ▪Creation of yaw moment corresponding to the control signals ▪Actuator displacement output
Sensor System Module	<ul style="list-style-type: none"> ▪Wheel/rail relative displacement measurement ▪Carbody vibration characteristic measurement ▪Yaw angle measurement of the steering bogie ▪Detection of the curve information ▪Wheel/rail dynamics monitoring

A. Active Steering Control Strategy

The basic concept of steering control strategy is to apply a controlled torque to the wheelset in the yaw direction. This can be achieved through longitudinal actuators as shown in Fig.2. This strategy is founded on the coupling of the lateral and yawing motions of the wheelsets by using the laser sensor signals represented in the wheel/rail displacement.

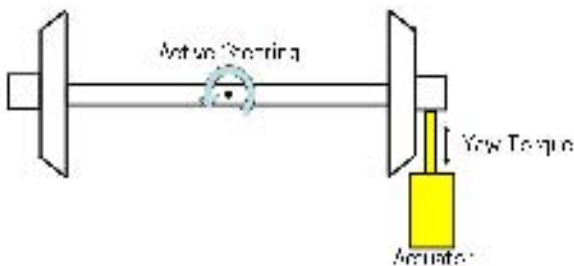


Fig.2 Active steering control strategy: longitudinal actuator method

As feedback signals, the relative movement between the wheels and the rail, called 'relative displacement', are considered in the development of controllers using the measured distance of the laser sensor from axle box to rail head.

B. Design of Active Steering Controller

The dSPACE system (DS1103 PPC Controller Board) is a powerful controller board for rapid control prototyping [32]. The PC runs the user interface and data logging code, and the DSP runs the real-time signal processing and analog I/O. The dSPACE has connections to MATLAB and Simulink. These connections allow a simulation on the PC and then run in real-time on the DSP. Fig.3 shows a realization of the active steering control module with MATLAB/ SIMULINK for a scale model.

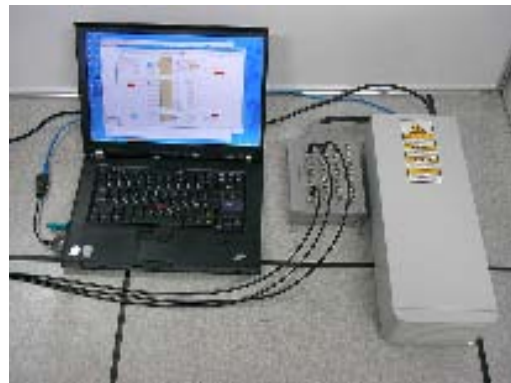


Fig.3 The dSPACE system (DS1103 PPC Controller Board)

Table II Specification of the DS1103 PPC Controller Board

Processor	Type	PPC 750GX
	Clock	1GHzCache
	Bus frequency	133MHz Memory
Memory	Local	32MB SDRAM
	Global	96MB SDRAM
ADC	Channels	16 multiplexed channels, 4 parallel channels
	Resolution	16-bit Output range
	Input range	± 10 [V]
DAC	Channels	8 channels
	Resolution	16-bit Output range
	Output range	± 10 [V]

The lateral displacements of front and rear axles are directly measured from four laser sensors. The center line of front and rear axles can be obtained as (1).

$$y_{front} = \frac{y_2 - y_1}{2}, y_{rear} = \frac{y_4 - y_3}{2} \quad (1)$$

where y_1 and y_2 mean laser sensor signals which is installed both ends of the front axle, y_3 and y_4 represent laser sensor signals which is installed both ends of the rear axle, and y_{front} and y_{rear} denote center lines of the front and rear axle.

The error signals can be obtained by calculating the difference between center lines and reference line, and used with input of the steering controller.

$$e = y_d - y \quad (2)$$

where y denotes a center line of the lateral displacement (i.e. y_{front} and y_{rear}) and y_d represents the reference lateral displacement which is calculated as (3).

$$y_d = \frac{r_0 l}{R \lambda} \quad (3)$$

where l denotes a half gauge of wheelsets ($=0.15$ [m]), r_0 represents a wheel radius ($=0.086$ [m]), and λ means a wheel conicity ($=0.2$).

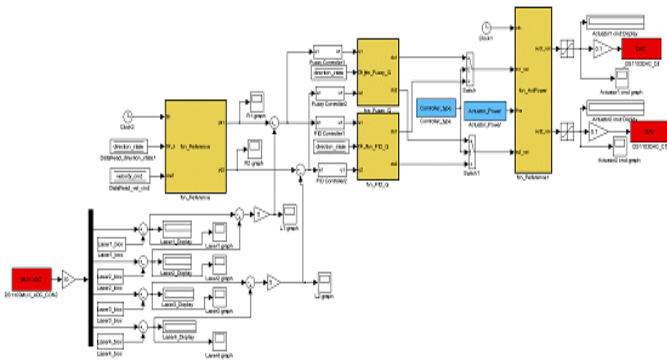


Fig.4 Realization of the active steering control module with MATLAB/SIMULINK

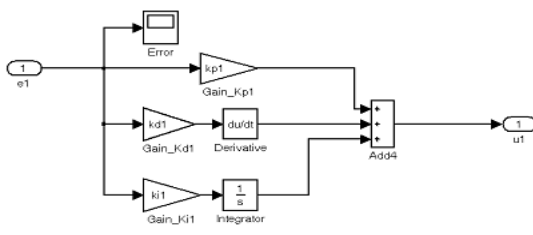


Fig.5 PID controller for active steering control with MATLAB/SIMULINK

Realization of the active steering control module with MATLAB/SIMULINK appears in Fig.4. The controller output $u(t)$ is calculated as (4).

$$u(t) = K_p e(t) + K_I \int_0^t e(\tau) d\tau + K_D \frac{de(t)}{dt} \quad (4)$$

The classic PI controller is applied to the active steering control as illustrated in Fig.5. The proportional gain $K_p = 0.9$ and integral gain $K_I = 0.9$ are used for two controllers with same values.

Table III Signal list for the active steering controller

Name		Range [v]	Physical	Input/Output
Driving Bogie Module	Velocity	0 ~ 5	0 ~ 3.9 [m/s]	Input
	Direction	0, 5	0: Forward 5: Backward	Input
	Braking	0, 5	0: 0 [N] 5: 18 [n]	Input
Steering Bogie Module	Actuator	-3 ~ 3	-3: -150[N] 3: 150[N]	Input
Data Acquisition Module	photoelectric sensor	0, 10	0, 10	Output
	Laser displacement sensor	-4 ~ 4	10 ± 4[cm]	Output
	Magnetic sensor	0, 10	0, 10	Output
	Gyroscope sensor	0 ~ 5	-100 ~ 100 [deg/sec]	Output
	Acceleration Sensor	0 ~ 4	0 ~ 4 [g]	Output
	Wireless Camera	-	320×240 [Pixel]	Output

Table III shows the signal list of the embedded system for the active steering controller which includes all the inputs and outputs that the embedded system has and describes their range, resolution, and so on.

III. EXPERIMENTAL ENVIRONMENT

A. Scale Railway Vehicle

Two axle bogies are used for the 1/5 scaled railway vehicle. A curve track with $R=20$ [m] and 27.11 [m] length is considered for a running test of the scale model. Fig.6 indicates the scaled railway vehicle composed of a driving bogie and a steering bogie, and test track.



Fig.6 Experimental environments (a scaled vehicle and a curved track)

B. BLDC Motor for Driving Bogie

For calculating the number of wheel rotation, we use a photoelectric sensor which is installed on the wheel in the driving bogie. Fig.7 shows the BLDC motor and for photoelectric sensor for calculating vehicle speed, and Fig. 8 indicates a pulse train generated from the photoelectric sensor.

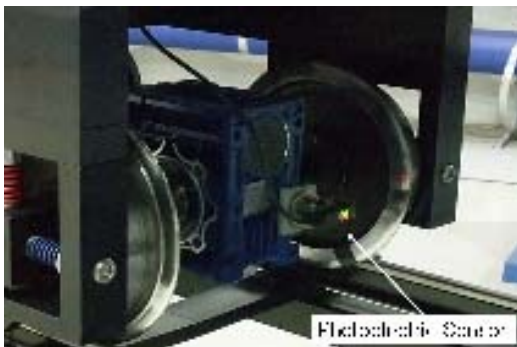


Fig.7 BLDC driving motor and photoelectric sensor for calculating vehicle speed

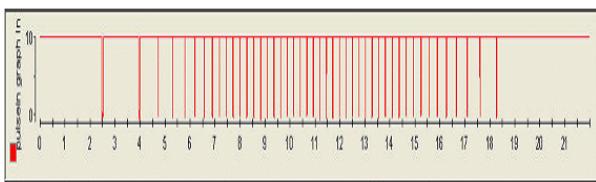


Fig.8 Pulse train for calculating the vehicle speed

The vehicle speed can be adjusted from 0 [m/s] to 3.8 [m/s] by changing of the input voltage between 0 [V] and 4 [V] at the control unit of the diving motor in the driving bogie. Fig.9 shows the load test results of the driving motor as velocity - voltage curve.

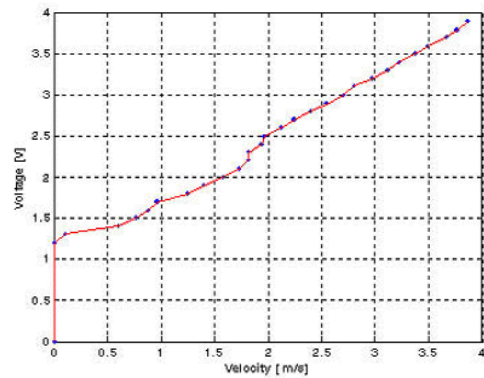


Fig.9 Load test results of the driving motor: velocity - voltage curve

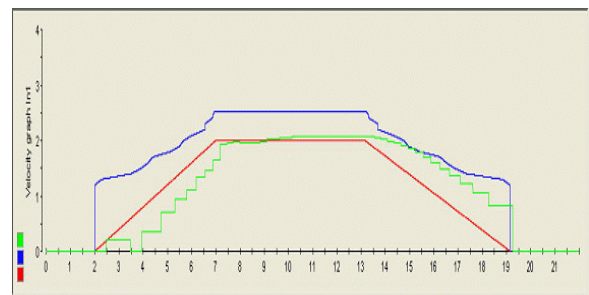
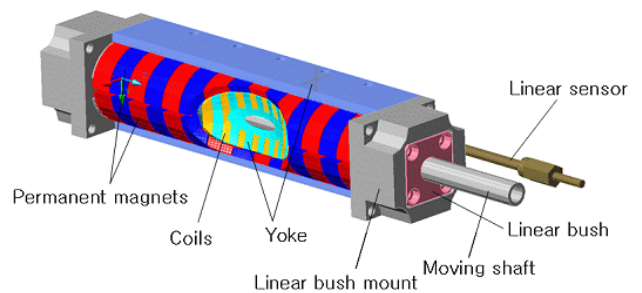


Fig.10 Velocity profile for driving bogie (red-line: the vehicle velocity profile [m/s], blue-line: the real voltage [v], green-line: the vehicle speed [m/s])

C. Actuator for Steering Bogie

The linear tabular motor is used for the actuator which can generate the yaw moment with control effort signals by using the measurement values of the relative lateral displacement between wheel and rail. The schematic view of linear tabular motor and the test product is depicted in Fig.11.



(a) Schematic view of linear tabular motor



(b) Linear tabular motor

Fig.11 Linear tabular motor of F-link type

The actuator force is proportional to the input voltage values as (5). That is, the actuator force increases linearly from 0 [N] to 200 [N] approximately proportionally to the actuator command voltage (0 [V] to 4 [V]).

$$F_{act} = 50 V_{com} \quad (5)$$

where F_{act} means a actuator force [N] and V_{com} represents a voltage command [V].

Table IV Specification of the linear tabular motor

Tubular Linear Motor	Size	70×70×230 [mm]
	Stroke Range	±30 [mm]
	Thrust	Continuous 200 [N]
Motor Driver	Input Voltage	24VDC (200W)
	Control type	3φ PWM Vector Control
	Driving Control	Force Control Mode
	Resolution	10μm

Table IV summarizes the specification of the linear tabular motor for generating steering force.

D. Measurement System for Scale Railway Vehicle

To detect the relative displacement between wheel and rail in the steering bogie, we utilize the four laser sensors. Fig.12 shows the shape of the laser sensors (Omron E3S-AD13 model) and mounted position.

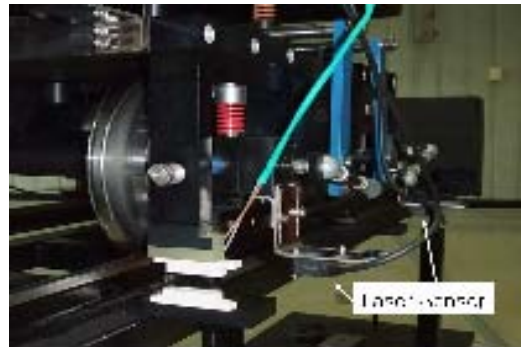


Fig.12 Laser sensors for measuring the relative displacement between wheel and rail

To measure the lateral force, one of the performance measures of the active steering system, the following measurement system which consists of strain gage sensors, a strain amplifier and a data acquisition system is used.

In addition, considering the control concept of the steering bogie, it coincides with an objective of active steering control in minimizing the lateral force which is calculated the absolute difference values between the front and rear wheel axis. Fig.13 indicates the lateral force measurement system using full bridge strain gage as a performance measure.

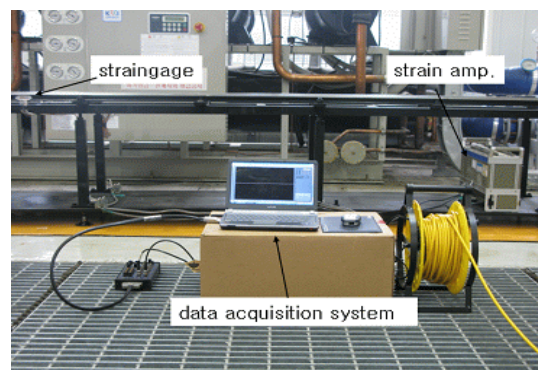


Fig.13 Lateral force measurement system using full bridge strain gage

IV. EXPERIMENT RESULTS

A. Experiment Results: Lateral Force

From Fig.14 and Fig.15, we can confirm that the lateral force is remarkably reduced under the active steering control.

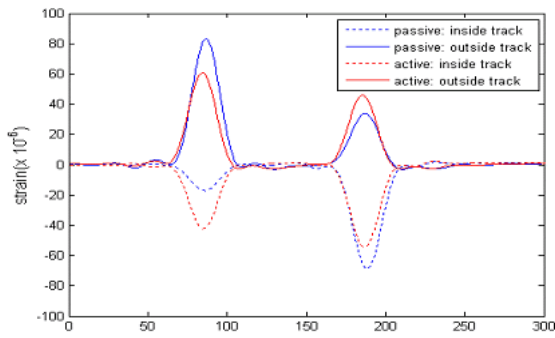


Fig.14 Experimental results: strain gage measured data

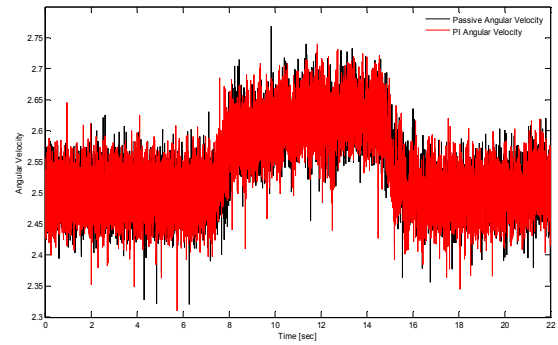


Fig.16 Experimental results: the gyroscopic sensor signals

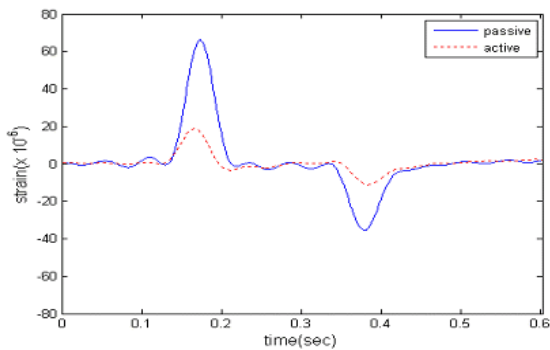


Fig.15 Experimental results: the absolute difference of lateral force between the front and rear wheel axis

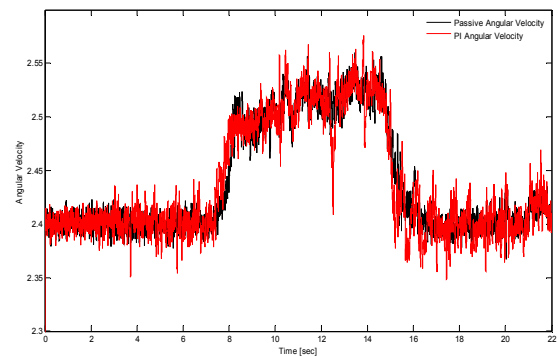


Fig.17 Experimental results: the gyroscopic sensor signals passed through the LPF

Compared with the passive system, the active steering control system outstandingly reduces the difference of lateral force 7.6 [μ] strains from 30.6 [μ] strain. Consequently this measurement of the difference of lateral force is able to confirm the lateral force reduction effect through track lateral force measuring system.

Table V The absolute difference between the lateral force value of the front axle and the rear axle

	No control	Active Control
Value	30.6 μ	7.6 μ

B. Experiment Results: yaw velocity

The lateral displacement as well as the actual curve radius is important signals from which the lateral dynamics of the vehicle can be observed. The actual curve radius can be estimated or measured by means of gyroscopic sensors. In order to analysis the yaw movement, a gyroscopic sensor (Silicon Sensing CRS03-02) which is mounted at the center of the steering bogie was used.

The gyroscopic sensor signals have been measured for the curve running of the passive system and the active system, respectively. Fig.16 shows the output signals of the gyroscopic sensor and Fig.17 indicates the output signals of the gyroscopic sensor passed through a low pass filter (LPF). To remove a high frequency noise from the gyroscopic sensor signals the noised signals were passed through a LPF such that its frequency response is equal to the response given by Fig.18 and Fig.19.

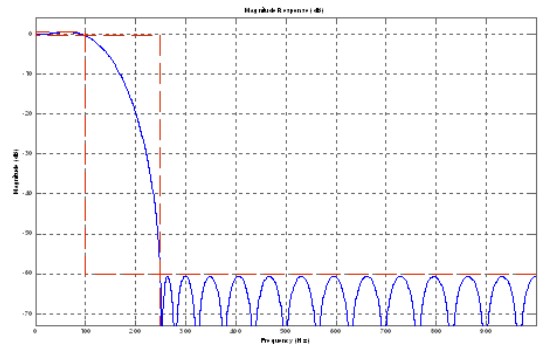


Fig.18 The frequency response of the LPF

The LPF which is composed of the FIR filter and is specified

as $F_s=2$ [kHz], $F_{pass}=0.1$ [kHz], $F_{stop} = 0.25$ [kHz], and $A_{pass} = 60$ [dB]. Graphically, the filter specifications look similar to shown in the following Fig.19.

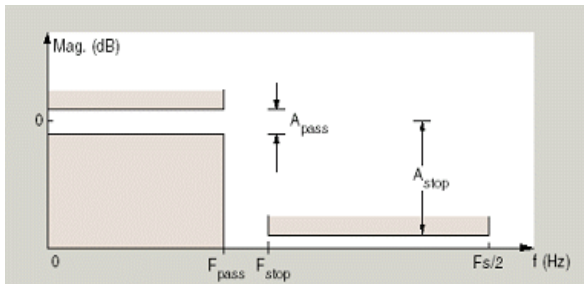


Fig.19 The filter design specifications of LPF

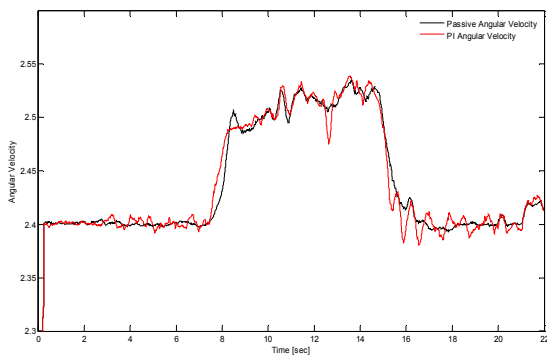


Fig.20 Experimental results: the gyrosopic sensor signals passed through the LPF and the moving average

To obtain more pure gyrosopic sensor signals the filtered signals is passed through a simple moving average with $k=256$ samples such as (6).

$$y_{MA}(n) = \frac{1}{k} \sum_{i=n-k+1}^n x(i) \quad (6)$$

Fig.20 shows the gyrosopic sensor signals passed through the LPF and the moving average. In Fig. 20 the gyrosopic sensor signal initially starts with 2.4[V] at the running of the straight track, then rotates clockwise 0.12[V] (or 4.8[°]) at the curving track. While moving a transition zone between a straight track and a curve track the rising time of the active steering system is faster than that of the passive system.

C. Experiment Results: Lateral displacement

Fig.21 shows the result of the relative lateral displacement in case of no steering control. The reference displacement of the front and rear axle is 3.085 [mm] as (3).

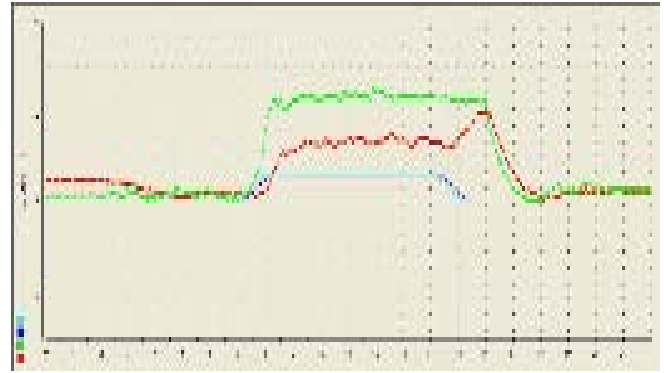


Fig.21 Experimental results: lateral displacement of no steering control (green-line: the front axle center line of the wheel/rail relative displacement [mm], red-line: the rear axle center line of the wheel/rail relative displacement [mm], cyan-line: reference displacement of the front axle [mm], blue-line: reference displacement of the rear axle [mm])

Fig.22 indicates the result of the relative lateral displacement in case of active steering control based on PI controller.

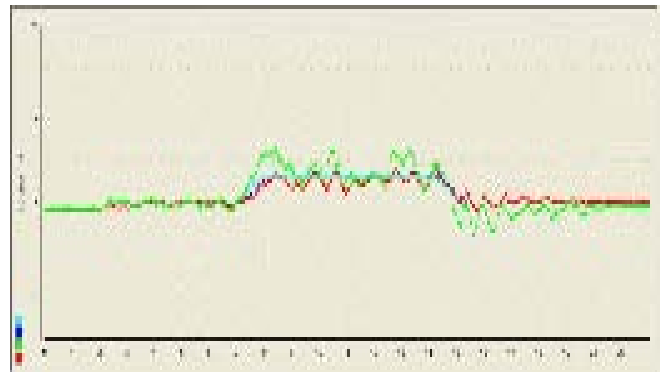
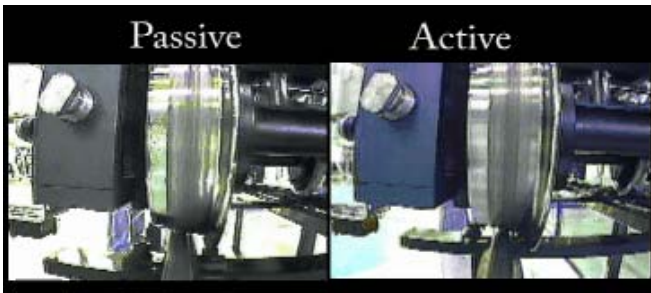


Fig.22 Experimental results: lateral displacement of active steering control (green-line: the front axle center line of the wheel/rail relative displacement [mm], red-line: the rear axle center line of the wheel/rail relative displacement [mm], cyan-line: reference displacement of the front axle [mm], blue-line: reference displacement of the rear axle [mm])

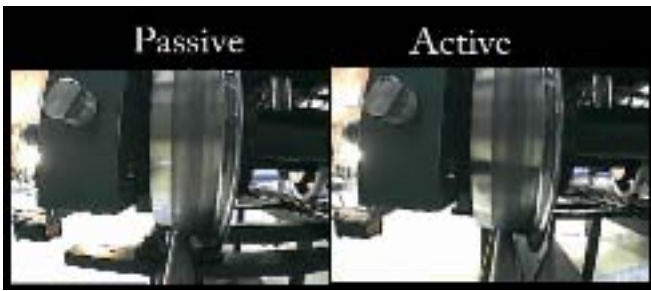
The experimental results of the active steering controller with the lateral wheel/rail displacement image using the 2.4 [GHz] wireless cameras are shown in Fig.23.



(a) Start position (time=0[sec])



(b) Curve position (time=10[sec])



(c) End position (time=20[sec])

Fig.23 Experimental results: wireless camera image of wheel/rail lateral displacement

D. Experiment Results: Actuator Command

The experimental results of the active steering controller with the actuator voltage are shown in Fig.24. As the Fig.24 indicates, a real actuator force of 150 [N] is applied to the wheelsets in case of 3 [V] actuator command voltage. The max actuator command voltage of the front axle is large values as 3 [v], in comparison with that of the rear axle as 2 [v].

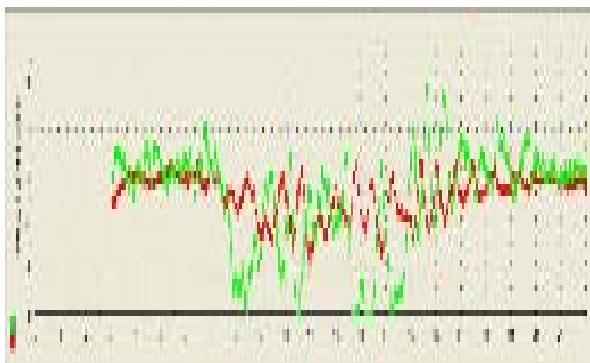


Fig.24 Experimental results: actuator command voltage graph of active steering control (green-line: the actuator command voltage of the front axle [V], red-line: the actuator command voltage of the rear axle [V])

E. Experiment Results: Relative Displacement Error

Fig.25 and Fig.26 shows the lateral displacement and the error responses ($y_d - y$) which are calculated as the difference between the relative lateral displacement (y), and the reference displacement (y_d).

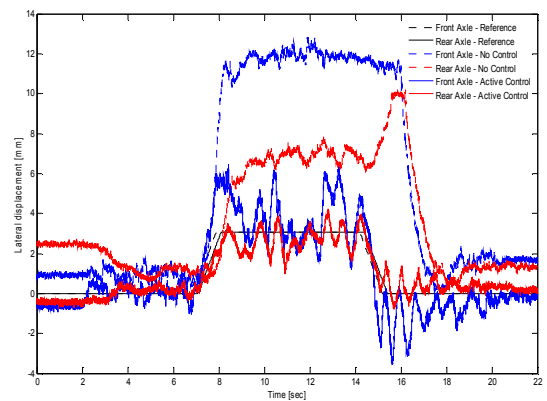


Fig.25 Experimental results: lateral displacement graph (dotted blue-line: the lateral displacement of the front axle in case of no control [mm], dotted red-line: the lateral displacement of the rear axle in case of no control [mm], solid blue-line: the lateral displacement of the front axle in case of active steering control [mm], solid red-line: the lateral displacement of the rear axle in case of active steering control [mm])

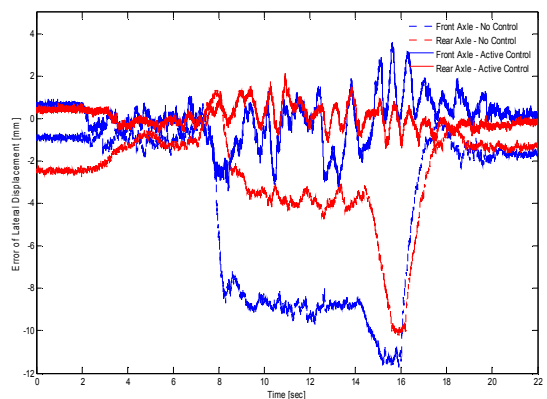


Fig.26 Experimental results: relative displacement error graph (dotted blue-line: the error displacement of the front axle in case of no control [mm], dotted red-line: the error displacement of the rear axle in case of no control [mm], solid blue-line: the error displacement of the front axle in case of active steering control [mm], solid red-line: the error displacement of the rear axle in case of active steering control [mm])

active steering control [mm], solid red-line: the error displacement of the rear axle in case of active steering control [mm])

MSE is used to evaluate the margin of the error, being given by

$$MSE = \frac{1}{(n-m+1)} \sum_{i=m}^n (y_d - y)^2, \quad (m < n) \quad (7)$$

where y denotes a center line of the lateral displacement and y_d represents the reference line.

Table VI Comparison of MSE (Mean Square Error) of the error signals over the interval between 4 [sec] to 20 [sec]

		No control	Active Control
MSE	Front Axle	44.5661	1.5550
	Rear Axle	14.3908	0.3036

Table VI summarizes the mean square value of the error signals, respectively. The error decreased by approximately from 3 times to 5 times.

V. CONCLUSION

Active steering system of railway vehicles is designed to alleviate wheel/rail contact forces and to decrease wheel/rail wear. In this paper, we present active steering controller design in the railway systems using classic PI controller. Control strategy to the active steering system based on two axle vehicle attached to actuator of the yaw torque considering the riding quality has been applied. Compared with passive system, experiment results have been shown that the proposed active steering control system outstandingly reduces the difference of lateral force and the mean square error of the front and rear axle.

For future research to the mechatronic vehicles, new suspension concepts should be considered offering more comfort, curving performance and running stability.

REFERENCES

- [1] Simon Iwnicki, *Handbook of Railway Vehicle Dynamics* (Eds), Taylor&Francis, 2006.
- [2] V. K. Garg, R. V. Dukkipati, *Dynamics of Railway Vehicle Systems*. Academic Press, 1984
- [3] A. Matsumoto, Y. Sato, "Multibody Dynamics Simulation and Experimental Evaluation for Active-Bogie-Steering Bogie," *Int. Symposium on Speed-Up and Service Technology for Railway and Maglev Systems*, 2006
- [4] J. Pérez, R. M. Goodall, "Control Strategies for Active Steering of Bogie-based Railway Vehicles," *Control Engineering Practice*, 2002.
- [5] J. T. Pearson, R. M. Goodall, "An Active Stability System for a High Speed Railway Vehicle," *Electronic Systems and Control Division Research*, 2003
- [6] Katsuya Tanifuji, "Active Steering of a Rail Vehicle with Two-Axle Bogies based on Wheelset Motion," *Vehicle System Dynamics*, 2003.
- [7] M. Athans, "The Role and Use of the Stochastic Linear-Quadratic-Gaussian Problem in Control System Design," *IEEE Trans. on AC*, 16(3), 1971
- [8] T.X. Mei, T.M. Goodall, "Recent Development in Active Steering of Railway Vehicles," *Vehicle System Dynamics*, 2003
- [9] Yoshihiro Suda, Takefumi Miyamoto, "Active Controlled Rail Vehicles for Improved Curving Performance and Response to Track Irregularity," *Vehicle System Dynamics Supplement*, 2001
- [10] S.Y. Lee and Y. C. Cheng, "Nonlinear Analysis Hunting Stability for High-Speed Railway Vehicle Trucks on Curved Tracks," *Vehicle System Dynamics Supplement*, Vol.127, 2005
- [11] H. Scheffel, R. D. Frohling, and P. S. Heyns, "Curving and Stability Analysis of Self-Steering Bogies Having A Variable Yaw Constraint," *Vehicle System Dynamics Proc. of 13th IAVSD Symp. on the Dynamics of vehicles on Roads and on Tracks*, Vol. 23(Suppl.), 1993, pp. 425-436
- [12] A. H. Wickens, "Static and Dynamic Stability of Unsymmetric Two-Axle Railway Vehicles Possessing perfect Steering," *Vehicle System Dynamics*, Vol. 11, 1982, pp. 89-106
- [13] A. H. Wickens, "Railway Vehicles with Generic Bogie Capable of Perfect Steering," *Vehicle System Dynamics*, Vol. 25, 1996, pp. 389-412
- [14] Y. Suda, T. Fujioka, and M. Iguchi, "Dynamic Stability and Curving Performance of Railway Vehicles," *130Bull. JSME*, 29(256), 1986, pp. 3538-3544
- [15] C. E. Bell, and D. Horak, "Forced Steering of Rail Vehicles: Stability and Curving Mechanics," *Vehicle System Dynamics*, Vol. 10, 1981, pp. 357-386
- [16] Y. Suda, "High Speed Stability and Curving Performance of Longitudinally Unsymmetric Trucks With Semi-Active Control," *Vehicle System Dynamics*, Vol. 23, 1994, pp. 29-51
- [17] T. Fujioka, Y. Suda, and M. Iguchi, "Representation of Railway Suspensions of Rail vehicles and Performance of Radical Trucks," *Bull. JSME* 27, 1984, pp.2249-2257
- [18] S. Narayana, R. V. Dukkipati, and M. O. M. Osman, "A Comparative Study on Lateral Stability and Steady State Curving Behavior of Unconventional Rail Truck Models," *Proc. Inst. Mech. Eng., F J. Rail Rapid ransit* 208, 1994, pp. 1-13
- [19] S. S. Marayana, R. V. Dukkipati, and M. O. M. Osman, "Analysis of modified Railway Passenger Truck Designs to Improve Lateral Stability/Curving Behavior Compatibility," *Proc. Inst. Mech. Eng., F J. Rail Rapid Transit* 209, 1995, pp.49-59
- [20] S. S. Marayana and R. V. Dukkipati, "Lateral Stability and Steady State Curving Behavior Performance of Unconventional Rail Trucks," *Mech. Mach. Theory* 36, 2001, pp. 577-587
- [21] R. V. Dukkipati, and S. S. Marayana, "Non-Linear Steady-State Curving Analysis of Some Unconventional Rail Trucks," *Mech. Mach. Theory*, 2001, pp. 507-521
- [22] R. V. Dukkipati, and S. S. Marayana, and M. O. M. Osman, "Curing Analysis of Modified Designs of Passenger Railway Vehicle Trucks," *JSME int. J., Ser. C* 25(1), 2002, pp. 159-167
- [23] G. Lorant, and G. Stepan, "The Role of Nonlinearities in the Dynamics of a single Railway Wheelset," *Machine Vibration* 5, 1996, pp. 18-26
- [24] T. Matsudaira, "Shimmy of Axle with Pair of Wheels," *Journal of Railway Engineering Research*, 1952, pp. 16-26
- [25] T. Matsudaira, N. N. Matsui, W. Arai, and K. Yokos, "Problems on Hunting of Railway Vehicle on Test Stand. Trans." *A.S.M.E Journal of Engineering In industry*, Vol. 91, Ser. B, no. 3, 1969, pp. 879-885
- [26] L. M. Sweet, J. A. Sivak, and W. F. Putman, "Non-linear Wheelset Forces in Flange Contact, Part I: Steady State Analysis and Numerical Results, Part 2: Measurement using Dynamically Scaled Models," *Journal of Dynamic Systems, measurement and Control*, Vol. 101, 1979, pp. 238-255
- [27] L. M. Sweet, A. Karmel, and S.R. Fairley, "Derailment Mechanics and safety Criteria for Complete Railway Vehicle Trucks," In: Wickens, A. (ed.): *The Dynamics of Vehicles on Roads and Tracks. PROC. 7TH IAVSD Symposium*, Cambridge, UK, 1981

- [28] A. Jaschinski, *On the Application of Similarity Laws to a Scaled Railway Bogie Model*, Dissertation, TU-Delft, 1990
- [29] M. Gretzschel and A. Jaschinski, "Design of an Active Wheelset on a Scaled Roller Rig," *Vehicle System Dynamics*, Vol. 41 No.5, 2004, pp. 365-381
- [30] M. S. Kim, Y. S. Byun, J. H. Park and W. H. You, "Active Steering Control of Railway Vehicles using Linear Quadratic Gaussian (LQG)," *The 2007 International Conference on Mechatronics and Information Technology*, Gifu, Japan, December, 2007
- [31] M. S. Kim, J. H. Park, H. M. Hur and W.H. You, "Design of Active Steering Fuzzy Controller for Railway Vehicles," *4th Asian Conference on Multibody Dynamics*, 2008
- [32] dSPACE, *Solution for Control*, 2007.
- [33] M. S. Kim, Y. S. Byun, Y. H. Lee and K. S. Lee, "Gain Scheduling Control of Levitation System in Electromagnetic Suspension Vehicle," *WSEAS Transactions on Circuits and Systems*, Vol.5, pp.1706-1712, 2006
- [34] M. S. Kim, Y. S. Byun, Y. H. Lee and K. S. Lee, "The Levitation Controller Design of an Electromagnetic Suspension Vehicle using Gain Scheduled Control," *5th WSEAS Int. Conf. on Circuits Systems, Electrics, Control & Signal Processing*, 2006.
- [35] M. S. Kim, Y. S. Byun and H. M. Hur, "Design of the Active Steering Controller of Scaled Railway Vehicle Improving Curving Performance," *The 7th WSEAS Int. Conf. on Circuits Systems, Electrics, Control & Signal Processing*, 2008
- [36] M. S. Kim, J. H. Park, and W. H. You, "Construction of Active Steering Control System for the Curving Performance Analysis of the Scaled Railway Vehicle," *The 7th WSEAS Int. Conf. on Circuits Systems, Electrics, Control & Signal Processing*, 2008